

# HYGRO-MECHANICAL MODELLING OF SELF INDUCED STRESSES: THE CASE OF VERCORS GUSSET

François Soleilhet, Farid Benboudjema, Xavier Jourdain, Fabrice Gatuingt

► **To cite this version:**

François Soleilhet, Farid Benboudjema, Xavier Jourdain, Fabrice Gatuingt. HYGRO-MECHANICAL MODELLING OF SELF INDUCED STRESSES: THE CASE OF VERCORS GUSSET. CONMOD 2018 International symposium on Concrete modelling, 2018, Delft, Netherlands. hal-02153141

**HAL Id: hal-02153141**

**<https://hal.archives-ouvertes.fr/hal-02153141>**

Submitted on 12 Jun 2019

**HAL** is a multi-disciplinary open access archive for the deposit and dissemination of scientific research documents, whether they are published or not. The documents may come from teaching and research institutions in France or abroad, or from public or private research centers.

L'archive ouverte pluridisciplinaire **HAL**, est destinée au dépôt et à la diffusion de documents scientifiques de niveau recherche, publiés ou non, émanant des établissements d'enseignement et de recherche français ou étrangers, des laboratoires publics ou privés.

# HYGRO-MECHANICAL MODELLING OF SELF INDUCED STRESSES: THE CASE OF VERCORS GUSSET

François Soleilhet <sup>(1)</sup>, Farid Benboudjema <sup>(1)</sup>, Xavier Jourdain <sup>(1)</sup> and Fabrice Gatuingt <sup>(1)</sup>

(1) LMT-Cachan/ENS—Paris—Saclay/CNRS/ Université Paris-Saclay, France

**Abstract ID Number (given by the organizers):** .....

**Keywords:** Drying, Shrinkage, Hydro-Mechanical Modelling, Cracked concrete

## Author contacts

Authors	E-Mail	Postal address
François Soleilhet	francois.soleilhet@ens-cachan.fr	61 av du Président Wilson 94230 Cachan
Farid Benboudjema	farid.benboudjema@ens-cachan.fr	61 av du Président Wilson 94230 Cachan
Xavier Jourdain	xavier.jourdain@ens-cachan.fr	61 av du Président Wilson 94230 Cachan
Fabrice Gatuingt	Fabric.gatuingt@ens-cachan.fr	61 av du Président Wilson 94230 Cachan

**Corresponding author for the paper:** François Soleilhet

**Presenter of the paper during the Conference:** François Soleilhet

Total number of pages of the paper (the first excluded):

11

## Instructions to authors submitting a final paper

Authors should submit a final paper corresponding to the accepted abstract **no later than 1 March 2018**. The organisers do not commit themselves to include in the Proceedings any paper received later than the above-mentioned deadline. At least one of the authors must register and pay his/her registration fee during the advance period (before May 1<sup>st</sup> 2018) for their paper to be included in the final programme of the Conference. In case an author has more than one paper, the registration would be valid only for one paper and co-author/s should be registered for publication of multiple papers.

This document provides information and instructions for preparing a paper to be included in the Proceedings of the ConMOD2018 Symposium. Papers and all related correspondences should be written in English.

In the manuscript, the paper article should be preceded by one page containing the author(s) information (as in this page). The page should contain the paper title, abstract ID number (given by the organisers), keywords, e-mail and postal address of each author. The first name will indicate the principal/corresponding author and those that follow, the co-authors in the order of precedence.

# HYGRO-MECHANICAL MODELLING OF SELF INDUCED STRESSES: THE CASE OF VERCORS GUSSET

François Soleilhet<sup>(1)</sup>, Farid Benboudjema<sup>(1)</sup>, Xavier Jourdain<sup>(1)</sup> and Fabrice Gatuingt<sup>(1)</sup>

(1) LMT-Cachan/ENS—Paris—Saclay/CNRS/ Université Paris-Saclay, France

## Abstract

The prediction of the concrete structure durability is closely linked to the prediction of cracking in the long-term. Initially saturated cementitious materials are the seat of water movement that are responsible for mechanisms such as drying shrinkage, creep or changes in mechanical properties. For instance, the differential drying between the surface and the core of the structure leads to a heterogeneous state of stresses and can induce significant micro cracking at the surface. Those micro-cracks will impact not only the mechanical properties but also the permeability of the structure [1]. In this study, a sequential analysis is proposed to represent the drying evolution and the corresponding cracking pattern. First, calculations are performed to model the drying process and to obtain relative shrinkage strains. These strains are, in a second step, applied in order to obtain the initial deflection and the cracking pattern. Then, the dried specimens can be subjected to various numerical tests in order to analyse the impact of drying effects on concrete mechanical properties even water permeability tests. The influence of shrinkage on cracking pattern due to the mechanical loading can also be investigated. A second part of this study is an application of the proposed modelling strategy to the first lift of the VeRCoRs containment wall mock up [2] (the gusset) in attempt to predict concrete cracking.

## 1. INTRODUCTION

Today, the durability of buildings is a major challenge. To address this problem it is necessary, among other things, to predict the long-term behaviour of the structures. Nevertheless, this task remains difficult. The great heterogeneity of the material combined with multiple origins of stresses (thermal, chemical, drying, mechanical) make the work complex.

The prediction of the concrete structure durability is closely linked to the prediction of cracking in the long-term. Initially saturated cementitious materials are the seats of water movements that are responsible for mechanisms such as drying shrinkage, creep or changes in mechanical properties. As the material dries, hydric gradients appear along the structure's thickness and create self-induced stresses. When these stresses overcome the tensile strength of the material cracking occurs. Those cracks will impact not only the mechanical properties but also the permeability of the structure [1]. In this study, a Hydro-Mechanical approach is proposed to represent the drying evolution and the corresponding cracking pattern in order to assess the risk of cracking in large structure. The first part of the paper deals with the description of the different parts of the model then the second part deals with an application of the model on the first level of the VeRCoRs containment wall (1:3 scale containment structure) [2], more specifically on the gusset of the structure. Modelling is conducted through CAST3M software [3].

## 2. NUMERICAL MODELLING

As part of the proposed work, some simplifying assumptions were made. The material is considered mature (final material properties) and hydration is not taken into account. All the mechanisms are considered in a decoupled way [4] which makes it possible to consider them one after the other.

### 2.1 Drying modelling

The drying of cement-based materials is a complex phenomenon. Several, more-or-less coupled, mechanisms are involved: permeation, diffusion, adsorption-desorption and condensation-evaporation. Drying can be analysed through the resolution of liquid water, vapour and dry air mass balance equations. The use of several hypotheses [5,6] allows for considering only the mass balance equation of liquid water:

$$\frac{dS_l}{dP_c} \frac{dP_c}{dt} = \text{div} \left( k_{rl}(S_l) \frac{K}{\mu_l \phi} \text{grad}(P_c) \right) \quad (1)$$

where  $S_l$ ,  $P_c$ ,  $\phi$ ,  $K$ ,  $k_{rl}$  and  $\mu_l$  are, respectively, the saturation degree, the capillary pressure, the porosity, the intrinsic permeability, the relative permeability and the viscosity of the liquid water. It is shown [8,9] that this equation is sufficient for an accurate prediction of the drying of ordinary and high-performance concretes at 20°C with a relative humidity greater than 50%. The capillary pressure and the relative permeability are related to the degree of saturation through van Genuchten's relations [7]:

$$S_l = \left( 1 + \frac{P_c}{P_0} \right)^{1-\gamma} \quad (2)$$

$$k_{rl}(S_l) = S_l^{n_k} \left( 1 - \left( 1 - S_l^{\frac{1}{\beta}} \right)^\beta \right)^2 \quad (3)$$

where  $n_k$ ,  $P_0$  and  $\beta$  are materials parameters. Drying at surfaces was modelled using a convection-type approach.

### 2.2 Drying shrinkage modelling

There are different ways to model drying shrinkage. Some of these are based on the theory of porous media mechanics. The development of this kind of modelling could be easily found in literature. See [8] for instance. Other models are based on phenomenological observations. Indeed, following experimental results [9,10] found a proportional relation between water content variation and drying shrinkage rate:

$$\underline{\dot{\epsilon}}_{ds} = k_{ds} \dot{w} \underline{\underline{1}} \quad (4)$$

where  $k_{ds}$  is a constant hydrous compressibility factor and  $\underline{\underline{1}}$  is the unit matrix. It is possible to find alternative approaches but in this present work this modelling approach was chosen. It is easy to implement and gives satisfactory results. Moreover, the modelling of the drying shrinkage takes into account basic and drying creep. This allows a relaxation of the stresses and then decreases of the damage induced by the drying gradients.

### 2.3 Creep modelling

Basic creep model used is a model of Burger with an aging dashpot (figure 1), more information are available in [11].

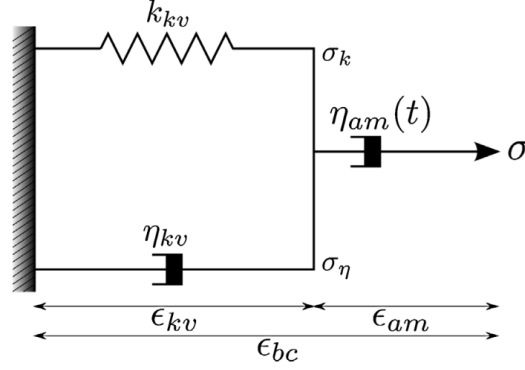


Figure 1: Rheological model for concrete basic's creep [11]

Thus without taking into account dissymmetric behaviour between tension and compression, the model is governed by the second order equation (5).

$$\frac{\dot{\sigma}}{k_{kv}} = \tau \ddot{\epsilon}_{kv} + \left(1 + \frac{k_{kv}}{k_{kv}}\right) \dot{\epsilon}_{kv} \quad \text{and} \quad \dot{\sigma} = \eta_{am} \dot{\epsilon}_{am} \quad \text{with} \quad \dot{\epsilon} = \dot{\epsilon}_{am} + \dot{\epsilon}_{kv} \quad (5)$$

This approach could be extended to three-dimensional problem using the behaviour law of the material.

Moreover, the drying creep is taken as an additional deformation [11]. The equation (6) links the evolution of drying shrinkage to the drying creep by a coefficient under stresses.

$$\dot{\underline{\epsilon}}_{dc} = \lambda_{dc} |\dot{\underline{\epsilon}}_{sh}| \sigma \quad (6)$$

where  $\lambda_{dc}$  is a constant  $\epsilon_{sh}$  is shrinkage deformation and  $\sigma$  is the stress applied.

### 2.3 Mechanical modelling

This study is based on 3D modelling. It involves non-explicit modelling of concrete cracking using a damage theory. The variable  $D$ , a scalar damage variable ranging from 0 to 1, is considered in the stress-strain relation:

$$\sigma_{ij} = (1 - D) C_{ijkl} \epsilon_{kl}^{elas} \quad (7)$$

where  $\sigma_{ij}$ ,  $C_{ijkl}$ ,  $\epsilon_{kl}^{elas}$ , are respectively stress, elastic stiffness and elastic strains. The evolution of the damage relies on an equivalent strain criterion, calculated from the equivalent strain  $\epsilon_{eq}$  introduced by Mazars [12]. It was shown [13] that the evolution of damage in tension could be taken as an exponentially decreasing:

$$D = 1 - \frac{\epsilon_{d0}}{\epsilon_{eq}} \cdot \exp\left(-B_t(\epsilon_{eq} - \epsilon_{d0})\right) \quad (8)$$

where  $\epsilon_{d0} = f_t/E_c$ , with  $f_t$  the tensile strength,  $E_c$  the Young modulus and  $B_t$  a parameter controlling the softening behaviour of the concrete.

Softening behaviour of concrete may lead to non-unity of solutions and mesh dependency. Energetic regularization prevents these difficulties [14]. Regularization is then based on the parameter  $B_t$ , which is a function of  $h$  the size of the finite element,  $f_t$  the tensile strength,  $G_f$  the fracture energy and a parameter for the initiation of the damage  $\epsilon_{d0}$  as described above.

$$B_t = \frac{h \cdot f_t}{G_f - \frac{h \cdot \epsilon_{d0} \cdot f_t}{2}} \quad (9)$$

Finally, a random field for the tensile strength generated by the Turning Band Method [15] is used in order to take into account the variability of the material. The chosen parameters are:

- A variation coefficient equal to 10 %;
- A correlation length three times larger than the biggest aggregate.

### 3. THE CASE OF VERCORS GUSSET

In this section we are interested in the containment gusset of the VeRCoRS project. To do this, a three-dimensional modelling of the reinforced concrete slab and the gusset is carried out.

#### 3.1 Meshes of the gusset

The invert and gusset are modelled using three-dimensional modelling. For reasons of cost calculation, modelling is only interested in a first approach at an angular sector of  $15^\circ$ . The mesh size is not much refined. It is composed of 3650 linear elements (figure 2c).

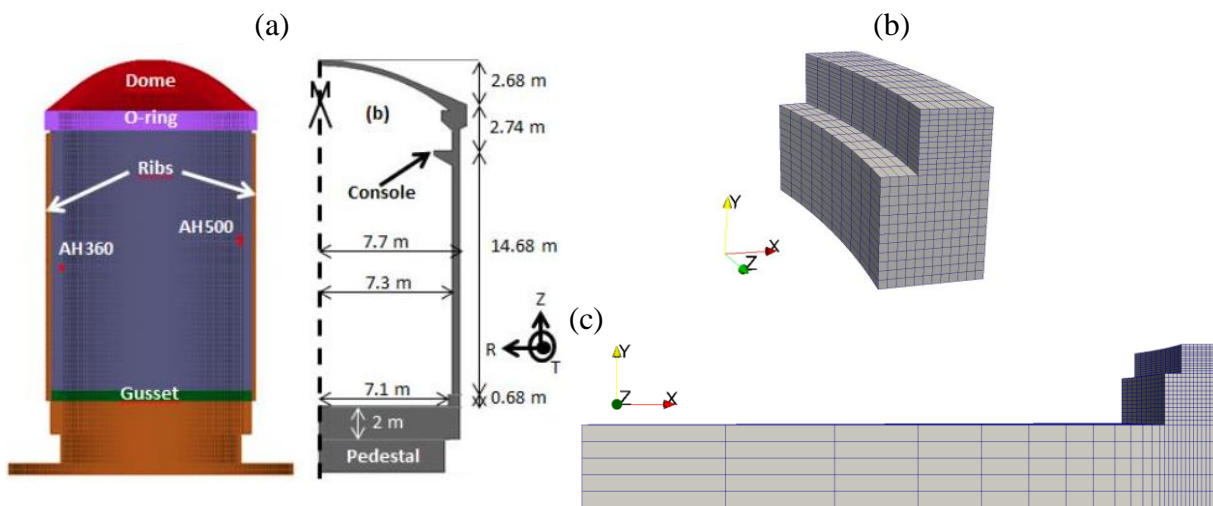


Figure 2: (a) General 3D and 2D-AXIS views of VeRCoRs mock-up [16], (b) 3D view of VeRCoRs gusset, (c)

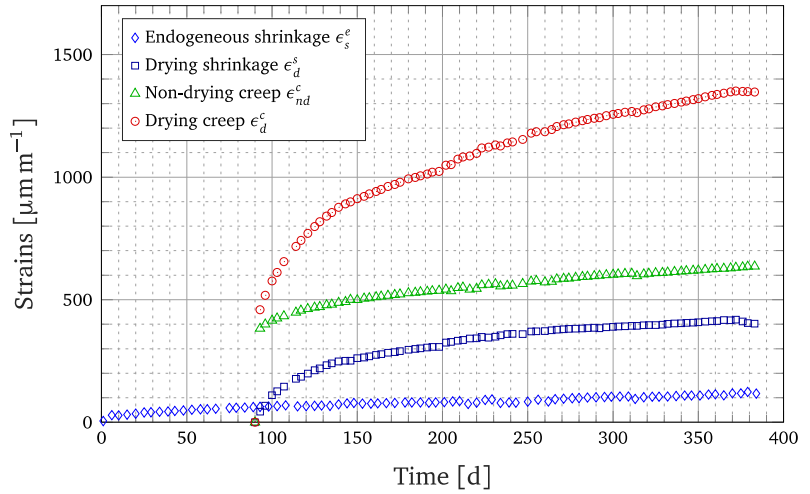
The primary interest of the modelling presented in this paper is the behaviour of the gusset (Figure 2b). For mechanical simulation, the axis of rotation of the containment wall is locked in the x and z directions. Movements normal to the side faces are locked.

### 3.2 Parameters' identification

To simulate the behaviour of the gusset, it is first necessary to identify the parameters of the Hydro-mechanical model. The latter are in numbers of 16. To do this, the relative mass variation of the specimen (16x100 cm) monitored by EDF [2] (Figure 3a) is identified on a 3D modelling of the cylindric sample to subsequently determine the different delayed strains presented on figure 2b.



(a)



(b)

Figure 3: Experimental characterization of delayed strains, (a) EDF experimental set up, (b) Experimental values measured on 16x100 cm sample [2]

Thus, on the basis of experimental data from the VeRCoRs project, it is necessary to first simulate the relative mass variation of the cylindrical sample in order to calibrate the various parameters of the hydro-mechanical model. The identified drying parameters are presented in table 1.

Table 1: Drying parameters of the model

$\beta$	$P_0$ [MPa]	$nk$	$K$ [ $\text{m}^2$ ]	$\Phi$	$\rho$ [ $\text{kg.m}^{-3}$ ]
0.42	25	-0.5	$1.5 \cdot 10^{-21}$	0.10	2400

The parameters in table 1 are used to simulate the evolution of the relative mass variation in a satisfactory manner. Over 600 days the mass loss is perfectly reproduced (cf. figure 4).

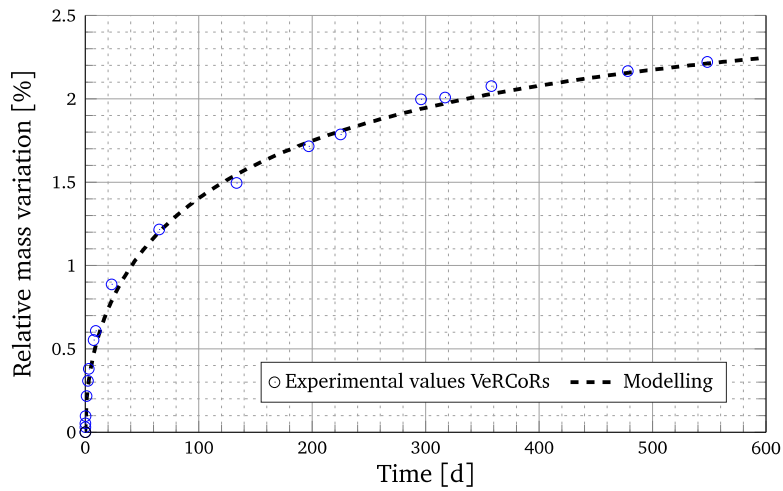


Figure 4: Relative mass variation of the cylindrical sample (16x100 cm) over 600 days and hydric prediction

Once the mass loss has been predicted it is possible to simulate the evolution of the drying shrinkage with equation (6) and an  $\lambda_{ds}$  equal to  $9.55 \cdot 10^{-6} \text{ m}^3 \cdot \text{L}^{-1}$ .

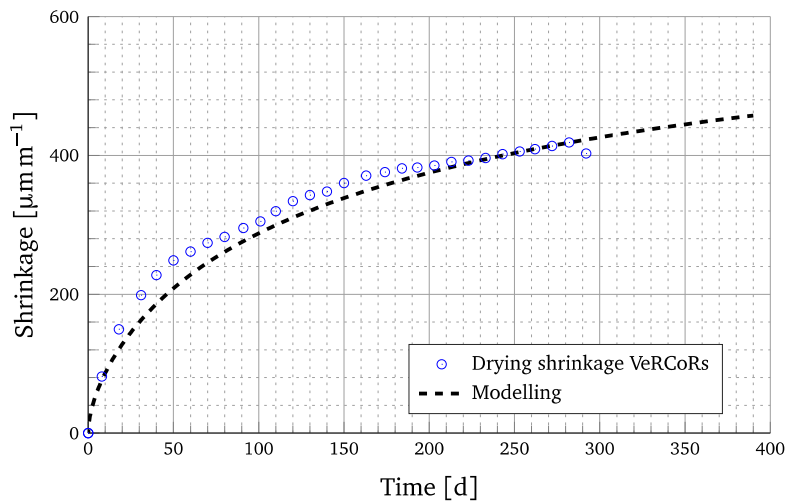


Figure 5: Evolution of drying shrinkage over time, experimental values and prediction

Figure 5 shows the evolution of drying shrinkage. Although relative mass variation is well predicted, it is difficult to simulate the evolution of drying shrinkage. The shrinkage value is slightly underestimated between 25 and 150 days and it can be assumed that in the longer term the shrinkage will be vaguely overestimated. Drying shrinkage prediction with capillary pressure models could be an interesting alternative. Nevertheless, for the purpose of this communication, the identification can be considered satisfactory.



Once the drying shrinkage is known, we can consider the experimental evolution of creep presented in the figure 3b. To do this, we simulate the basic creep under a load of 12 MPa and finally the total creep. The resulting curves are shown in Figures 6a and 6b.

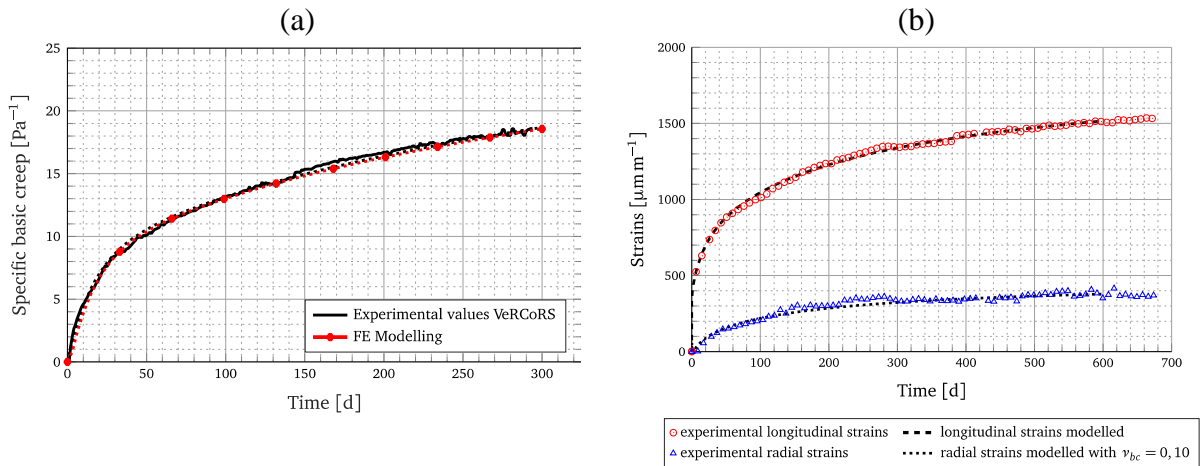


Figure 6: Identification of creep parameters, (a) Specific basic creep, (b) Total creep, longitudinal and radial strains

All curves shown in Figure 6 are correctly reproduced after 600 days of loading. By using a creep Poisson ratio coefficient equal to 0.10 it is possible to reproduce the radial behaviour of cylindrical specimens. Thus the creep parameters can be summarized in table 2.

Table 2: Parameters of drying shrinkage, basic and drying creep

$t_0$ [day]	$\eta_{am}$ [GPa.s <sup>-1</sup> ]	$k_{kv}$ [GPa]	$\tau_{kv}$ [day]	$\nu_{bc}$ [-]	$\lambda_{dc}$ [MPa]
90	130	135	15	0.10	$7.24 \cdot 10^{-2}$

Finally, the average mechanical parameters used in modelling are taken equal to those obtained on site for this area of the structure. These are summarized in Table 3. EDF Lab obtained the mechanical parameters on laboratory samples. No size effects were taken into account in the first approach.

Table 3: Mechanical parameters

$E$ [GPa]	$\nu$ [-]	$f_t$ [MPa]	$G_f$ [J.m <sup>-2</sup> ]	$\beta$ [-]
32.3	0.24	4.2	75	1

### 3.3 Drying

We can now focus on invert and gusset modelling. Thereafter, only the gusset will be studied although the whole will be modelled. For drying simulation, the parameters in Table 1 are used. Moisture conditions are imposed on the inner and outer surfaces of the structure. As shown in Figure 7a, conditions are considered constant at first approach and equal to 30% RH indoor and 50% RH outdoor.

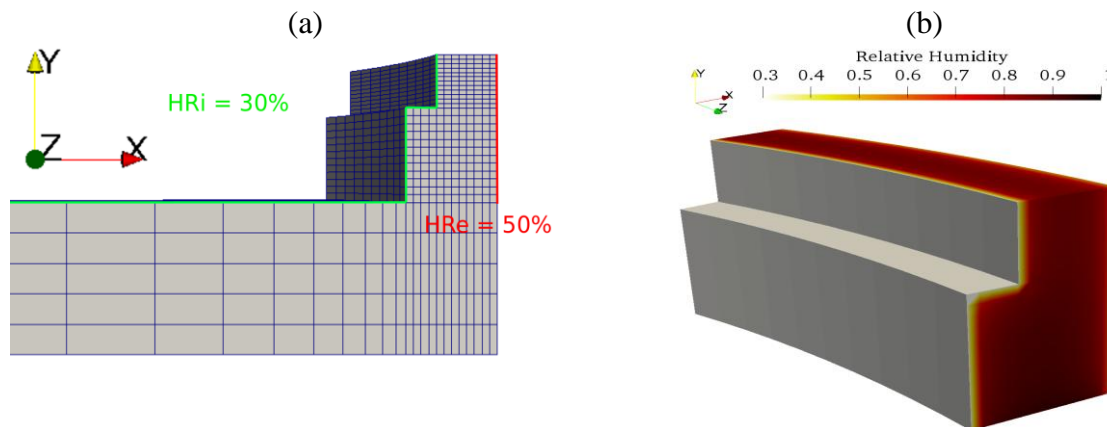


Figure 7: Drying modelling of the gusset, (a) Hydric condition, (b) Relative humidity fields after 8 years

The relative humidity field is thus simulated over a period of 3000 days or approximately 8 years. Figure 7b shows the relative humidity distribution within the gusset at the end of the simulation. It can be seen that the relative humidity on the exchange surfaces is close to the conditions imposed and that the heart of the gusset is still very humid (relative humidity close to 80%). Furthermore, it is difficult to capture drying gradients due to the coarse mesh size.

### 3.4 Mechanical analysis of the gusset

In this last part, the mechanical simulation of the gusset is performed. Figure 8 shows the deformation after 3 days. There is a rotation from the outer surface to the inner surface. This deformation is essentially explained by the difference in conditions at the limits imposed on the inside and outside. Indeed, the serviceability conditions (30% RH here) are more severe than the external ambient conditions (for this simulation 50% RH), which generate a greater shrinkage of the internal face and thus generates bending at the gusset.

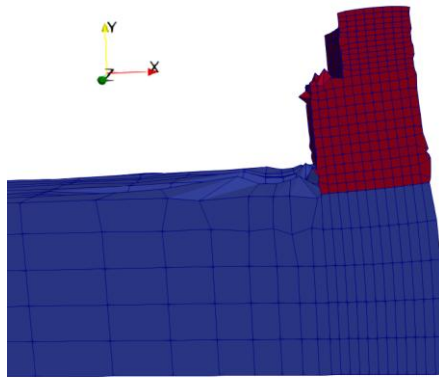
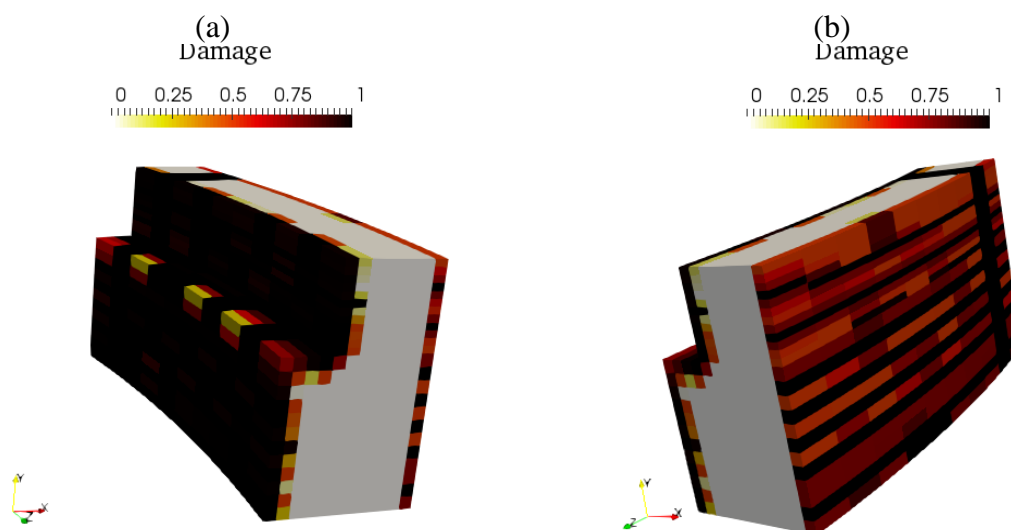


Figure 8: Deformation of the invert and the gusset after 4 years (amplification factor of 500)

If we now look at Figures 9, which show the damage on both sides of the gusset, we see that the damage is diffuse on the exchange sides. The latter is located in the first band of elements in contact with the drying conditions; here the band is about 5 cm. On the inner part (figure 9a) the damage is generally close to 1. Conversely on the external side, the values oscillate between 0.5 and 1. The random field generates areas of greater damage (Figure 9b), which concentrates the crack in these areas. On the other hand, Figure 9c shows through damage at the junction between the gusset and the invert. This last, strongly more massive than the gusset will generate a lower drying shrinkage what will restrict the shrinkage of the gusset and thus generate this strong damage. In addition, there is a severely damaged through one vertical slice of the gusset in Figure 9b. These damage map results together illustrate the significant impact of drying.



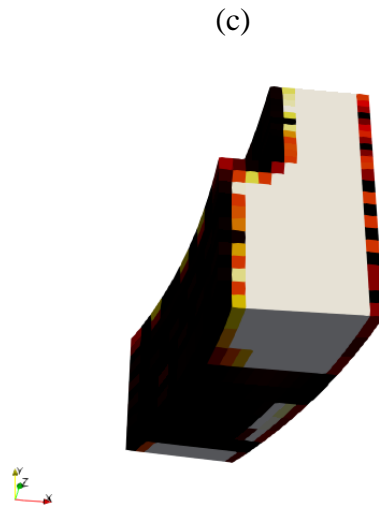


Figure 9: Damage on the gusset after 8 years, (a) Inner surface, (b) outer surface, (c) view from under

#### 4. CONCLUSIONS

The coupling between the hydric evolution of the material and its mechanical behaviour is of major importance for predicting the durability of a structure. In this paper a hydro-mechanical model was developed. The different parts of the model were described and then the modelling of the gusset of VeRCoRs containment wall was discussed. After calibrating the hydro-mechanical model parameters on experimental data provided by EDF LAB, a  $15^\circ$  angular sector of the gusset was simulated using a three-dimensional modelling. Hydric fields have been predicted and show that after 3000 days, the gusset is still not in equilibrium with its surrounding environment. The mechanical simulation showed a rotation of the gusset towards the inside of the structure, which is quite characteristic of containment structures since internal conditions are more severe than external conditions. Finally, the damage observed in these first simulations is diffuse on the surface and the random field favours areas of greater damage. In the proposed simulation we observe a through damage at the foot of the gusset and on one slice of the gusset. Finally, the mechanical simulations presented are promising and need to continue in this direction.

#### ACKNOWLEDGEMENTS

The authors are grateful to EDF for the provided in situ measurements.

## REFERENCES

- [1] Yurtdas, I., Peng, H., Burlion, N. and Skoczylas, F., 'Influences of water by cement ratio on mechanical properties of mortars submitted to drying', *Cement and Concrete Research* **36** (2006) 1286-1293.
- [2] Corbin, M. and Garcia, M., Benchmark VeRCoRs report 2015 ([www.conference-service.com/edf-VeRCoRs/welcome.cgi](http://www.conference-service.com/edf-VeRCoRs/welcome.cgi)).
- [3] Cast3m® software: <http://www-cast3m.cea.fr>
- [4] Granger L. 'Comportement différé du béton dans les enceintes de centrales nucléaires : analyse et modélisation.', Thèse de doctorat de l'École Nationale des Ponts et Chaussées (1995).
- [5] Bažant ZP, Sener S, Kim JK, 'Effect of cracking on drying permeability and diffusivity of concrete'. *ACI Materials Journal* **84**, (1986) 351--357
- [6] Hansen TC, 'Creep of concrete: the influence of variations in the humidity of ambient atmosphere', Proceedings 6th Congress of the International Association of Bridge and Structural Engineering, Stockholm, (1960) 57-65.
- [7] Lassabatère, T. and , Torrenti, J-M and Granger, L., 'Sur le couplage entre séchage du béton et contrainte appliqué', Proceedings Actes du Symposium Saint-Venant, Paris, (1997) 331-338.
- [8] Thiery, M., Baroghel-Bouny, and al., 'Modélisation du séchage des bétons : analyse des différents modes de transfert hydrique', *Revue Européenne de Génie Civil* **11**, (2007) 541—577.
- [9] Goltermann, P., 'Mechanical predictions of concrete deterioration – Part 2: classification of crack patterns', *ACI Materials Journals* **92**, (1995) 58-63.
- [10] Baroghel-Bouny V, Mainguy Mand and al., 'Characterization and identification of equilibrium and transfer moisture properties for ordinary and high-performance cementitious materials', *Cement and Concrete Research* **29**, (1999) 1225-1238.
- [11] Hilaire, A., Benboudjema, F., Darquennes, A., Berthaud, Y., and Nahas, G., 'Modeling basic creep in concrete at early-age under compressive and tensile loading'. *Nuclear Engineering and Design* **269**, (2014) 222-230.
- [12] Mazars J. 'A description of micro-and macro scale damage of concrete structures'. *Eng Fract Mech* **25**, (1986).
- [13] Feenstra PH. 'Computational aspects of biaxial stress in plain and reinforced concrete', PhD thesis Technical University of Delft (1993).
- [14] Hillerborg A, Modéer M, Petersson P-E., 'Analysis of crack formation and crack growth in concrete by means of fracture mechanics and finite elements. ', *Cem Concr Res* **6**, (1976) 773–81.
- [15] Matheron, G, 'The intrinsic random functions and their applications', *Advances in applied probability*, (1973) 439-468.
- [16] Bouhjiti, E. M., Briffaut, M., Baroth, J., Dufour, F. and Masson, B., 'Thermo-mechanical modelling of the early age behaviour of concrete in Nuclear Containment Buildings', *Proceeding of the 2<sup>nd</sup> International RILEM/COST Conference on Early Age Cracking and Serviceability in Cement-based Materials and Structures*, (2017) 647-652.